INTERSPIKE-INTERVAL FLUCTUATIONS

IN *APLYSIA* PACEMAKER NEURONS

DOUGLAS JUNGE *and* GEORGE P. MOORE

From the Department of Physiology and Brain Research Institute, University of California, Los Angeles. Dr. Junge's present address is: the Marine Neurobiology Facility, UCLA Brain Research Institute and Physiological Research Laboratory, Scripps Institution of Oceanography, La Jolla, California.

ABSTRACT   In recent years, several mathematical models have been put forth to explain the time sequence of spike discharges in single neurons, in terms of synaptic inputs or intrinsic mechanisms. All of these models have been hypothetical, in that intracellular events were assumed, and not measured directly. The purpose of the present work was to study the statistics of the discharge from a preparation where intracellular recording was possible, and relate the observed discharge to measurable cell parameters. Regularly firing "pacemaker neurons" in the visceral ganglion of *Aplysia californica* were studied, using intracellular stimulating and recording techniques. Measurements were obtained of average curves of membrane potential, threshold for spike initiation, membrane resistance, and fluctuations of potential in the intervals between spontaneously occurring spikes. The timing of discharges from these neurons was described quantitatively by interspike-interval histograms, mean and standard deviation of intervals, skewness, and serial correlation coefficients. A mathematical model (contained in a simulation program for the IBM 7094 computer) was constructed, based on discrete fluctuations of membrane potential following each spike and other directly observed intracellular events. It was found that the model could quantitatively account for observed spike trains, including variations in the discharge from one cell to another.

INTRODUCTION

The attempt to delineate mechanisms which determine the time of firing of single neurons is especially difficult in the mammalian nervous system. The small size of many of the cells involved makes the intracellular monitoring of synaptic input or other fluctuations of membrane potential far more difficult technically than the extracellular recording of spike activity. Consequently, a number of studies have been published (for review, see Moore et al., 1966) which seek to infer, from a statistical analysis of the spike trains themselves, the input and/or intrinsic intracellular determinants of the observed discharge (Hagiwara, 1954; Viernstein and Grossman, 1961; Amassian et al., 1962; Fetz and Gerstein, 1963; Gerstein and

Mandelbrot, 1964; Weiss, 1964; Goldberg et al., 1964; Bishop et al., 1964; ten Hoopen 1964 and 1966; Stein, 1965; Verveen and Derksen, 1965; Buller, 1965; Geisler and Goldberg, 1966). The models proposed have been probabilistic in that fluctuations of intervals between spikes were attributed to random variations of the membrane potential, resulting from random arrivals of synaptic input or intrinsically "noisy" membrane processes (Fatt and Katz, 1952). All of the studies published to date have been based on extracellularly recorded spike data, and have therefore been hypothetical as to their assertions concerning input and/or intrinsic fluctuations of membrane potential.[1]

The motivation for the present work was thus to bridge the gap between inferential models applied to extracellular spike data and the basic electrophysiology which is known for many large single neurons. We wished to study the statistics of the discharge from a neuronal preparation where intracellular recording was possible. A model could then be constructed, based on direct measurements of cell parameters and intrinsic fluctuations of potential.

The visceral ganglion of *Aplysia* proved to be a convenient preparation for this study, for two main reasons: (*a*) many of the cells in the ganglion have relatively large diameters (50 to 200μ), and are easily penetrated with microelectrodes, and (*b*) these neurons are very hardy and will continue to discharge for hours after impalement. Hence, it is possible to obtain relatively longer spike trains for analysis than are available, for instance, in rapidly adapting sensory receptors (Buller, 1965). Many of the few hundred cells in the ganglion show spontaneous activity, with or without postsynaptic potentials visible in the intracellular records (Tauc, 1960). We decided to restrict our observations, initially at least, to the so-called "pacemaker neurons" which comprise at least 10% of the autoactive cells. These neurons discharge very regularly, and apparently do not receive any synaptic input, detectable as postsynaptic potentials in intracellular recordings or sudden variations in the mean rate of firing. Hence, pacemaker neurons afford the added opportunity to evaluate the statistics of the spike generating mechanism itself, uncomplicated by synaptic input to the cell. (This type of study is a necessary preliminary to a model which includes the effects of input.)

MATERIALS AND METHODS

The visceral ganglion of *Aplysia californica* was isolated and maintained in natural sea water. The temperature of the bath was in the range 12°-16°C, and was maintained constant to within 1° during each experiment. The periganglionic connective tissue sheath was opened in the region of the giant neuron (Arvanitaki and Chalazonitis, 1958) where preliminary exploration revealed a high density of the desired pacemaker neurons.

---

[1] The only single neuron model based on intracellular data which we have found is reported in the note of Calvin and Stevens (1965), referring to the interspike-interval distributions of some repetitively discharging motoneurons.

Practically all of the experiments to be described were performed on cells in this region (a few pacemaker neurons were studied near the origin of the branchial nerve).

The electrodes used were of the conventional glass capillary type, filled with 3M KCl, whose resistances were 5 to 20 meg. A Medistor model A-35 electrometer amplifier was employed, and its output was fed into a Tektronix Model 502 oscilloscope. Electrical activity was also displayed on a Grass polygraph and recorded on an Ampex model 354 tape recorder, using a Mnemotron FM converter. Intracellular stimulation was applied through a separate intrasomatic electrode.

Selection and Processing of Data. Since our purpose was to study purely autogenous neuronal activity, the first criterion applied to the electrical records was freedom from synaptic input. Recording was confined to regularly discharging cells, and polygraph records were examined to exclude spike trains showing any postsynaptic potentials.

Aplysia neurons in general show a gradual slowing of discharge rate throughout the period of recording, possibly because of initial irritation as a result of impalement. Rather than attempting to analyze this trend and including it in the model, we chose to select sequences which showed minimal slowing, and treat them as stationary. For this sorting process, tachograms were made of all the recorded sequences, where the size of the interval preceding each spike was represented as the length of a vertical line (produced by resetting a linear ramp generator with each spike). A sample tachogram is shown in Fig. 1, for a sequence of 200 intervals. This cell shows a typical amount of slowing and fluctuation of intervals. The criterion which was adopted for acceptance of sequences was that the *means* of the first and last ten intervals should not differ by more than the *range* of the first ten. It was found, using this procedure, that standard deviations of whole sequences were usually within a factor of two of the SD's of the ten interval samples. This method of selection was used for two principal reasons: (*a*) slowing did not always occur at a constant rate, and would be difficult to correct for, and (*b*) SD's of the whole sequences, chosen in this way, were sufficiently precise to permit compari-
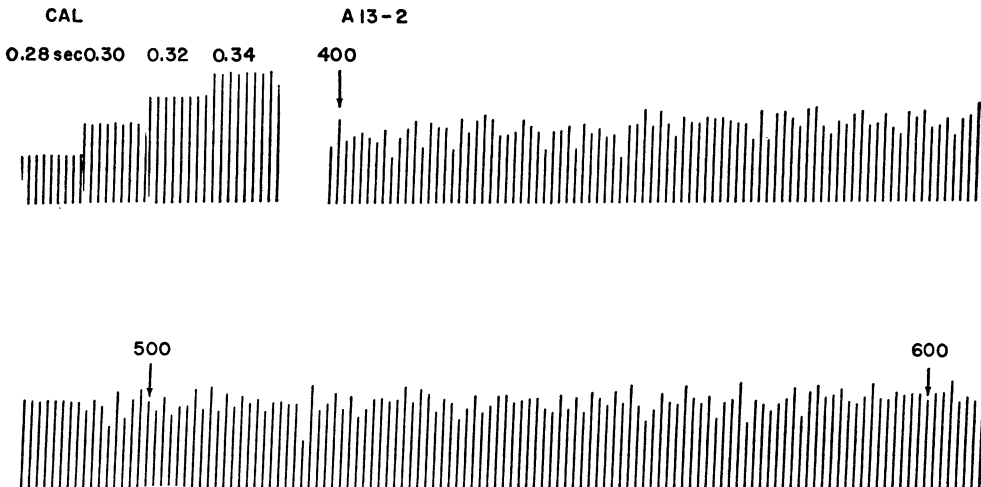

FIGURE 1 Tachogram, where the duration of each interval is represented as the length of a vertical line. Spontaneous sequence is shown from interval 400 to interval 600. Method described in text.

sons between different spike trains, where standard deviations varied over a large range (0.0019 to 0.2048 sec). Sixty three sequences were chosen for analysis on this basis. Several cells were examined for over an hour, during which time they underwent slow changes in rate; in some cases, two or more sequences were taken from the same cell firing at different mean rates.

Spike trains which met the above criteria were digitized in the data processing laboratory of the UCLA Brain Research Institute. Rectangular pulses were produced each time the spike potentials exceeded a preset level, and the intervals between pulses were measured to the nearest 0.667 msec. Lists of the consecutive intervals were then written on digital tapes, which were analyzed by a statistical program for the IBM 7094 computer (Perkel, 1965). This program calculated interspike-interval histograms, mean interval, standard deviation, coefficient of variation (=SD/mean), skewness of the histograms, and serial correlation coefficients between lengths of successive pairs of intervals.

RESULTS

A. Intracellular Events During the Pacemaker Cycle

Membrane potential. Typical intracellular potential records from pacemaker neurons, presumably firing in the absence of synaptic input, are shown in Fig. 2. Following each spike is a slow depolarization, which brings the membrane potential to the threshold level, initiating the next spike. This drift of potential between spikes will be referred to as the "pacemaker potential." The spike may or may not be preceded by a smaller elevation (Fig. 2e), which is thought to be due partly to the electrotonically conducted axon spike, and partly to a somatic "local response" (Tauc, 1962a). Axon excitation is considered to precede and initiate somatic firing in *Aplysia* neurons (Tauc, 1962b), and pacemaker activity can occasionally continue in the absence of somatic invasion (Fig. 2f).

In many of the cells examined, the shapes of the pacemaker potentials between spikes could be fitted quite closely by exponentials of the form $V = V_R (1 - e^{-t/\tau})$, where the zeros of potential and time were taken at the point of maximum undershoot. The method of fitting consisted of estimating a value of V_R by inspection, and plotting measured values of $\ln(V_R - V)$ against t on semilogarithmic paper. The straight line determined by observation to fit this data then had a slope of $-1/\tau$. Fig. 3 shows a comparison of a real pacemaker potential and an exponential curve, represented by the heavy dots.

Three types of deviation from exponentiality were occasionally seen: (a) some pacemaker potentials showed upward concavity immediately before each spike (Fig. 2c). Though lacking direct proof, we felt it was reasonable to assume that this concavity represented a contribution of the axon spike and somatic local response to the record, and was not a characteristic of the basic pacemaker process. (b) Other pacemaker potentials had a rapid exponential recovery followed by a long segment with constant rate of depolarization (Fig. 2e). This behavior was suggestive of a two-component process, such as a rapid somatic afterpotential superim-
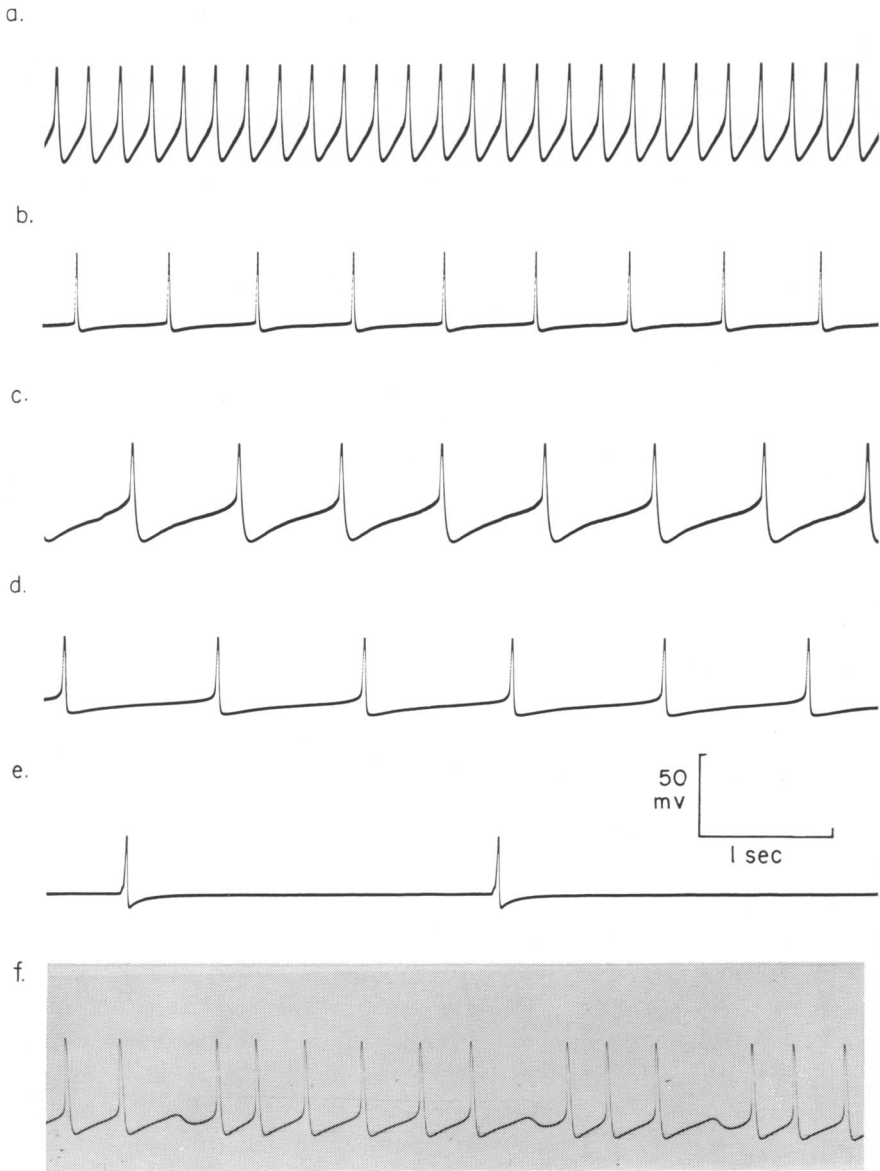
FIGURE 2 Intracellular records of spontaneous activity in six different "pacemaker neurons." Recording electrodes in cell somata. In each record, positivity is upward, and the zero of transmembrane potential is slightly below the peaks of the spikes. In *e*, effects of axon spikes are visible immediately before the somatic spikes. In *f*, failure of somatic invasion is seen; repolarization presumably due to axon spike.
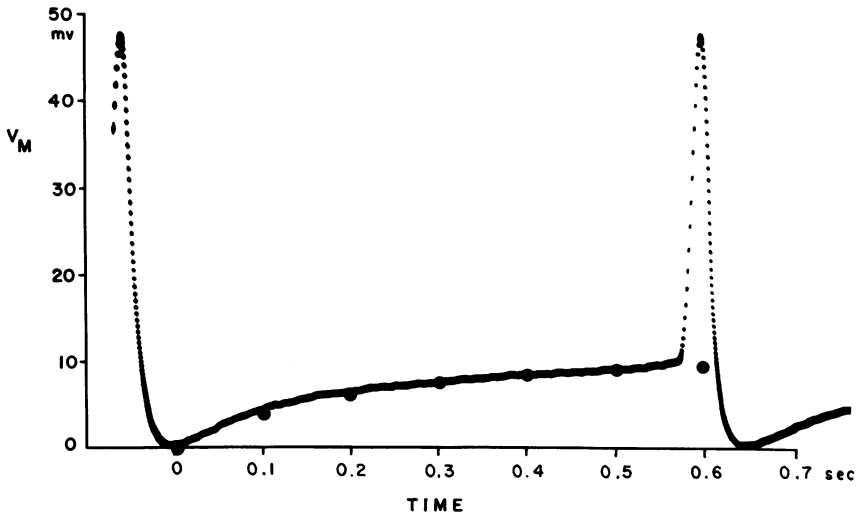
FIGURE 3 Comparison of observed pacemaker potential (solid line) and exponential curve (heavy dots). Method of fitting to exponential described in text. Dots on spikes introduced by FM tape recording system.

posed on a slower depolarizing drift due to leakage. (c) Some potential curves were nearly linear between spikes (Fig. 2a). These, too, were fitted with exponentials, by assuming a large asymptotic potential and large time constant.

Since many of the observed pacemaker potentials could be described by exponential curves, we wished to determine if any consistent variation in the parameters of the exponential equation occurred between cells firing at different mean rates. It was expected, for example, that the threshold potential, as measured from the undershoot, might be inversely correlated with mean rate. However, we found that, while many fast cells (2/sec or more) did have small thresholds (3 to 15 mv), an equal number had large values (15 to 25 mv). Slow cells (1.5/sec or less) in general had medium or small thresholds (15 mv or less).

Membrane resistance. Since it has been suggested (Lewis, 1965) that pacemaker activity might be a result of time-varying conductance changes, we wished to determine by direct measurements if any significant changes occurred in the membrane resistance during the period between spikes. A constant-current pulse was applied through an electrode inserted into the soma, while the intracellular potential was observed through another electrode impaling the same cell. A spontaneous spike was used to trigger the pulse, after an adjustable delay. The height of the depolarization produced by each pulse was proportional to the membrane resistance. In Fig. 4, the second spike in each trace is seen to be more or less accelerated by this procedure, depending on the time of application of the pulses. In this cell, the membrane resistance may have been slightly lower immediately after
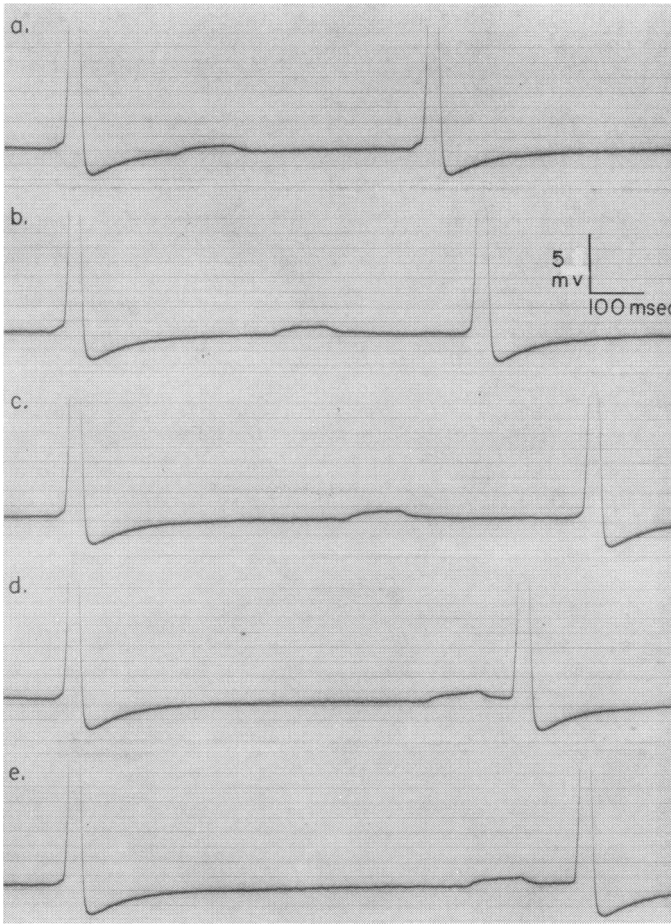
FIGURE 4 Membrane resistance measured at different times after the spike. Small depolarization between spikes in each record is produced by a constant-current pulse; height of the depolarization is proportional to membrane resistance. Method described in text.

the spike than later, but no large variations were seen. In four other cells examined in this way, it was also found that the membrane resistance reached a constant level early in the pacemaker cycle.

Fluctuations of potential. In order to account for irregularity of the discharge in the absence of synaptic input, a single-neuron model must be in part probabilistic. Most models to date have assumed continuous random fluctuations of membrane potential as the intrinsic source of arrhythmicity of firing, although extracellular recording was used in these studies, and membrane potentials were not actually measured. Membrane potential noise has usually been assumed to be

band filtered in frequency, with Gaussian amplitude distribution (Hagiwara, 1954; Viernstein and Grossman, 1961; ten Hoopen, 1964; Weiss, 1964; Buller, 1965; Geisler and Goldberg, 1966; Verveen and Derksen, 1965). We wished to determine, from intracellular recordings, the nature of the principal fluctuations of potential in *Aplysia* neurons. In these experiments, particular care was given to the elimination of 60 cycle/sec hum and vibration artifacts from the records. With the electrode in the sea water bath, the over-all drift of the recording system was less than 0.5 mv/10 min, and the amplifier noise was estimated to be 0.05 mv rms.

The variability of the pacemaker potentials was studied in superimposed oscilloscope traces, as shown in Fig. 5. The sweep was triggered when the spike potential exceeded a preset level, and the sweep speed was adjusted to display only two spikes. (Trigger stability is indicated by the constant potential at which the first spikes arise, and by the close superposition of first spikes.) In this way, every other pacemaker potential appeared in the photograph. Fig. 5f shows a display using expanded voltage and time scales, where the sweep was triggered by the same
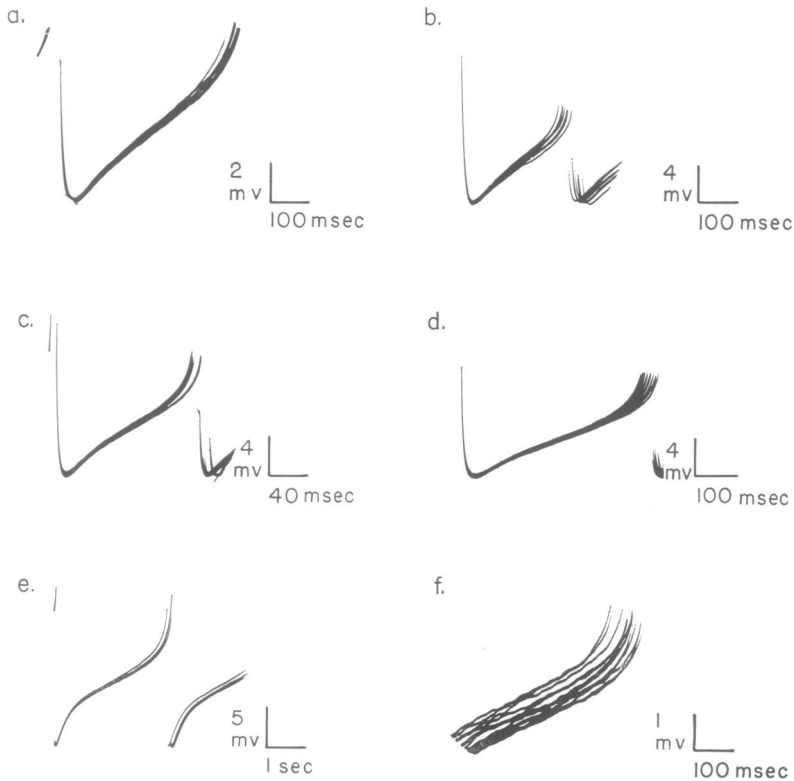

FIGURE 5 Superimposed pacemaker potentials. Oscilloscope sweep triggered by every second spike. Parts *a* through *e*, undershoot and two spikes visible in record. Part *f* triggering by same method, but voltage and time scales expanded.

method (the lower portions of the curves are cut off by the edge of the oscilloscope screen). One striking feature of these records was the considerable extent to which successive pacemaker potentials did not overlap or cross one another. The pacemaker curves were observed to occur in a random order, but the most negative curves were always associated with the longest intervals, and the least negative with the shortest intervals (see especially Fig. 5f). Some overlapping of potentials did occur between spikes, but such small fluctuations could be attributed to the inherent noise level of the recording system (about 0.05 mv rms). Thus, to within experimental error, the pacemaker potentials were different from one interval to another; i.e., they tended not to have the same values at any phase of the cycle. This suggested that the principal fluctuations of potential from cycle to cycle were not produced by a continuous noise process, but were due to a discrete random resetting of a cell parameter, such as membrane resistance or charging current, following the spike. This interpretation will be continued in the Discussion.

A quantitative description of these potential fluctuations was obtained from photographs with the oscilloscope graticule illuminated, to show voltage and time scales. Four consecutive photographs were taken, each containing five superimposed pacemaker potentials, where the sweep was triggered by every other spike. It was thus possible to construct histograms of membrane potential at fixed times following the spike, consisting of 20 measurements each. In Fig. 6 values of SD_V, the standard deviation of potential, are plotted against time after the spike at which the histograms
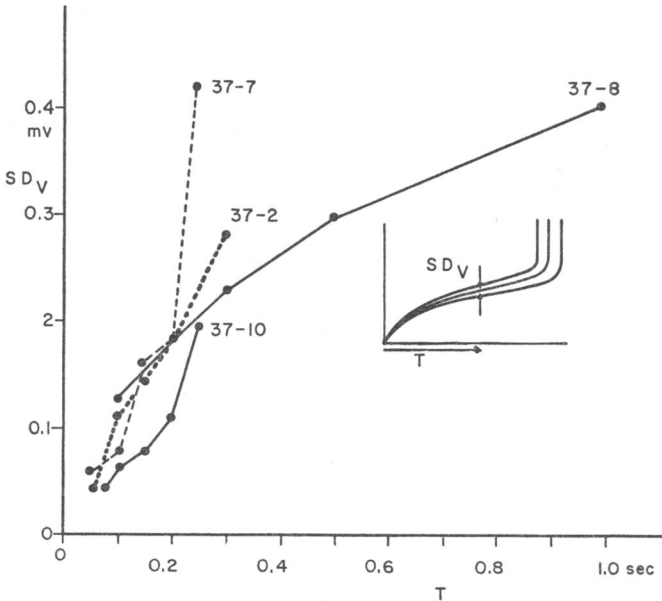

FIGURE 6 Standard deviation of membrane potential as a function of time after the spike. Standard deviation of undershoot is shown by the first point in each curve.

were obtained, for four cells. The undershoot, indicated by the first point in each curve, always showed the least fluctuation. This eliminated a slow base line drift as the source of dispersion of potentials during the pacemaker cycle. The small fluctuation of the undershoot probably contributed to the values of SD_V during the cycle. The time course of the growth of SD_V was comparable in all four cells; at the same time in each pacemaker cycle, values of SD_V did not differ by more than about a factor of two. The largest standard deviations, just prior to the next spikes, had a range of 0.2 to 0.6 mv.
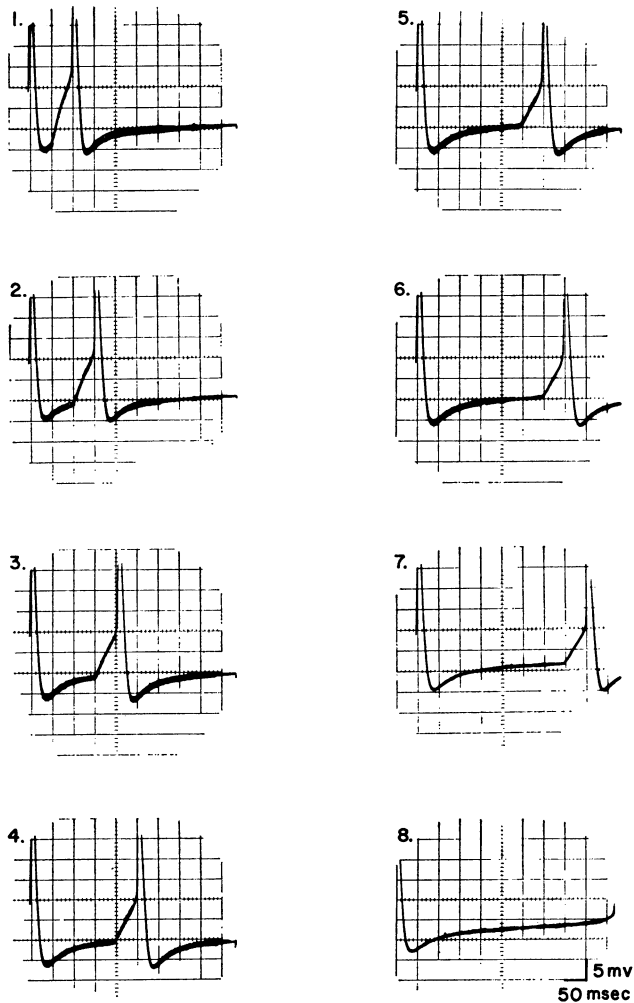

FIGURE 7 Threshold level of membrane potential for spike initiation, as a function of time after previous spike. Criterion for spike initiation was that second spike must occur promptly at the end of the stimulating pulse. Spontaneous interspike interval shown in 8. Method described in text.

Threshold. In the statistical models of single-neuron activity thus far proposed, spikes are assumed to arise when the membrane potential exceeds a threshold value, usually measured from the resting potential. Threshold has been assumed to have a constant value between spikes (Viernstein and Grossman, 1961; Amassian et al., 1962; Fetz and Gerstein, 1963; Gerstein and Mandelbrot, 1964; Bishop et al., 1964; Stein, 1965; Verveen and Derksen, 1965; ten Hoopen, 1966), or to follow a downward curve of recovery after each spike (Hagiwara, 1954; Weiss, 1964; ten Hoopen, 1964, Buller, 1965; Geisler and Goldberg, 1966). The curves of threshold in these models were inferential (i.e. they could not be measured by the extracellular recording methods used). We wished to determine the time course of recovery of threshold in *Aplysia* pacemaker neurons by direct methods.

Two aspects of the firing threshold were investigated: (*a*) using a two-electrode preparation, the recovery of threshold was measured as a function of time after the spike. Spontaneous spikes from the recording electrode were used to trigger a constant-current pulse. After an adjustable delay, this pulse was reapplied to the soma through the stimulating electrode. Thus, at several different delays after the spike, threshold was measured as the level to which the membrane potential had to be raised, by adjusting the current, in order to cause a spike promptly at the end of the pulse. Fig. 7 shows the result of one such experiment: the oscilloscope sweep was triggered by the first spike which appears at the left. In parts 1 through 7, the pulse was delivered later and later after the spike; a spontaneous interspike interval is shown in part 8. [The elevation of the threshold to brief pulses above that for spontaneous spikes is a result of the remoteness of the spike-initiating region (Tauc, 1962*b*)]. It was seen that the level of potential necessary to produce a second spike promptly at the end of the pulse was slightly elevated at the smallest delays, but had a constant value throughout most of the pacemaker cycle. This result was obtained for several other cells; however, in a few cases, the threshold declined continuously throughout the cycle. (*b*) We also examined the effects on the threshold of maintained outward currents applied to the soma through a second electrode, causing an increase in the rate of discharge. Here again threshold was defined as the level of membrane potential at which the spikes occurred. Fig. 8 shows the result of this procedure in a different cell from that considered above. In parts *a, b,* and *c,* maintained currents of increasing strength were applied at about the center of the trace. The principal effect was to increase the slope of the pacemaker potential. Even when a large change in firing rate was produced, the critical level for spike initiation remained relatively constant. On the basis of this observation and that presented in Fig. 7, it was concluded that a model assuming a constant threshold between spikes could adequately describe a class of pacemaker neurons.

B. Statistics of the Observed Time Intervals between Spikes

Interspike-interval histograms. These were obtained for 63 spike trains.
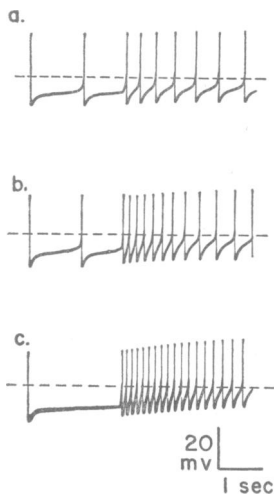
a.

b.

FIGURE 8 Effect of maintained dc stimulation applied through second intrasomatic electrode. Spontaneous activity on left side of each record. Stimulation starts approximately at center of each record, and continues beyond the visible portion. Spikes retouched; method described in text.

c.

20 mv

1 sec

$$SD = K (\bar{T})^{1.21}$$

0.2 SEC

S D

0.15

0.1

0.05

0.4   0.6   0.8 SEC

2.2   2.4   2.6 SEC

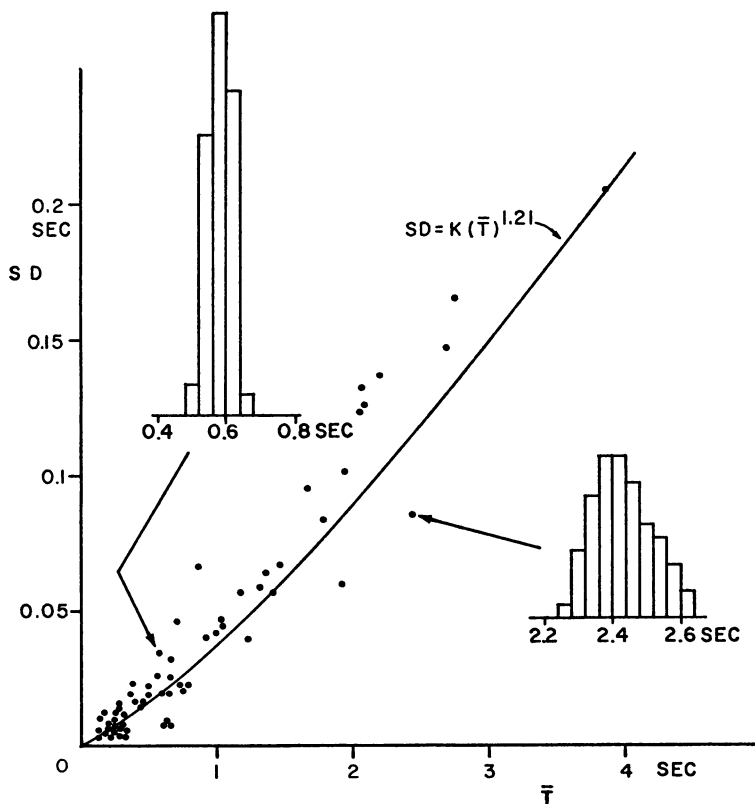O   1   2   3   4   SEC

$\bar{T}$

FIGURE 9 Standard deviation of intervals versus mean interval, in 63 spontaneous spike trains. In some cases, two or more spike trains taken from the same cell, firing at different mean rates. Solid line shows power function of best fit to the data (method of fitting described in text). Inserts show typical histograms.

In some cases, two or more histograms were taken from the same cell firing at different mean rates. The inserts in Fig. 9 show typical histograms from two different cells, plotted with common time scales and bin-widths. In general, all of the histograms appeared normal in shape on first inspection; mean intervals were close to the modes, and the tails were not markedly asymmetrical. These cells discharged quite regularly; standard deviations were only 1% to 8% of the mean intervals. Fig. 9 also shows a plot of mean interval on abscissa and SD on ordinate, for all 63 cases studied. Standard deviation was strongly correlated with mean, despite the fact that most samples came from different cells. The variation of SD with mean could be described by the power function SD $= 0.00944 \ (\bar{T})^{1.21}$, shown by the solid line. [The fitting procedure consisted of plotting log SD versus log $\bar{T}$, and finding the straight line of best fit by the least squares method (Hoel, 1962, p. 177)]. The strong dependency of SD upon $\bar{T}$ was shown by the correlation coefficient of the log data, which was 0.92.

The use of a power function to relate SD and mean of interval histograms from *different* cells has been studied explicitly by some workers (Buller, 1965; Biederman, 1965). This type of function also gives a good description of the variation of SD with mean in *single* cells discharging at different mean rates (Table I). In human muscle spike records, however, the data show strong curvature when plotted on log-log paper (Tokizane and Shimazu, 1964). Hagiwara (1954) has pointed out that, in general, the finding of strongly correlated SD and mean may be explained by assuming that both quantities are principally determined by a single parameter, which varies from histogram to histogram. It will be shown in the Discussion that

TABLE I

STANDARD DEVIATION VS. MEAN INTERVAL IN SINGLE CELLS AT
VARIOUS MEAN RATES

Source	Preparation	Standard deviation as function of mean	Range of means
		msec	*msec*
Junge, 1965	Visceral ganglion of *Aplysia*	$0.00944 \ (\bar{T})^{1.21}$	127–3860
Biederman, 1965	Crayfish ventral nerve cord	$0.001 \ (\bar{T})^{2}$	30–600
Hagiwara, 1954	Toad spindle afferents	$0.0295 \ (\bar{T})^{1.47}$	9–221
Buller et al., 1953	Frog spindle afferents: Fast cells	$0.00261 \ (\bar{T})^{2.03}$	6–350
	Slow cells	$1.00 \ \bar{T}$	350–2000
Goldberg et al., 1964	Superior olivary complex (cat):		
	Fast cells type I	$1.00 \ \bar{T}$	4–54
	Fast cells type II	$0.0836 \ (\bar{T})^{1.54}$	4–45
	Slow cells	$0.00159 \ (\bar{T})^{2.03}$	26–124
Werner and Mountcastle, 1963	Ventrobasal thalamus (monkey):		
	Spontaneous	$1.52 \ \bar{T} - const.$	30–70
	Driven	$0.63 \ \bar{T}$	10–52

this assumption can provide an adequate description of the variation of SD with mean in our population of pacemaker neurons.

The skewness of the interval histograms was calculated from the third moment about the mean (Weast, 1964–65). Skewness varied from −1.1 to +0.74, with 87% of the values between −0.4 and +0.4. No definite correlation could be seen between skewness and mean interval from one cell to another.

Independence of intervals. Serial correlation coefficients (Hoel, 1962, p. 163) were calculated between the adjacent intervals T_{i+1} and T_i (r_1), and between the separated intervals T_{i+4} and T_i (r_4). Values of r_1 ranged from −0.051 to +0.888, with a mean of +0.293; r_4 varied from −0.174 to +0.757, with a mean value of +0.266. Although no test was made, both r_1 and r_4 were thought to be significantly positive in most cells. However, as mentioned earlier, these neurons underwent a very gradual slowing of discharge rate throughout the recording period. This slowing was probably the main source of the observed dependency, and would be expected to produce correlation between widely spaced intervals as well as between adjacent intervals. Sequences of spikes were selected according to the previously stated criterion for stationarity, but this criterion was not sufficiently restrictive to eliminate positive correlation. However, since the dependency was produced by slowing, and was not a functional property of the spike generating process itself, it was considered irrelevant to a representative model. A renewal process, where successive intervals were independent (Cox and Lewis, 1966), could give an adequate description of the observed firing patterns, if it accounted for the shapes of the interval histograms and the variations of the histograms with different mean intervals.

Variations of standard deviation with mean interspike interval in single cells. Changes in mean rate were induced in single pacemaker neurons by passing maintained currents through a second intrasomatic electrode. It was shown earlier that this procedure changed the slope of the pacemaker potential, without greatly altering the firing threshold (Fig. 8). Observed differences in the firing patterns of one cell under varying amounts of dc stimulation are shown in Fig. 10. Histogram 1 is spontaneous, 2 is produced by an outward current through the cell membrane, 3 is spontaneous, 4 is produced by an inward current, and 5 is spontaneous. The ordinate is given as a probability density, to compensate for the unequal sample sizes. In the insert is shown the standard deviation of intervals at each mean (solid line), and the SD-mean curve for the entire population of cells (dashed line). In this and other neurons examined in this way, standard deviation was strongly correlated with mean interval. For this particular cell, the SD-mean curve was similar to that describing the whole population; in other cells the two curves were less alike. However, the finding of dependency of SD upon mean interval could be explained by the previously mentioned assumption that both quantities were determined by a single parameter, which varied with the amplitude of stimulation.
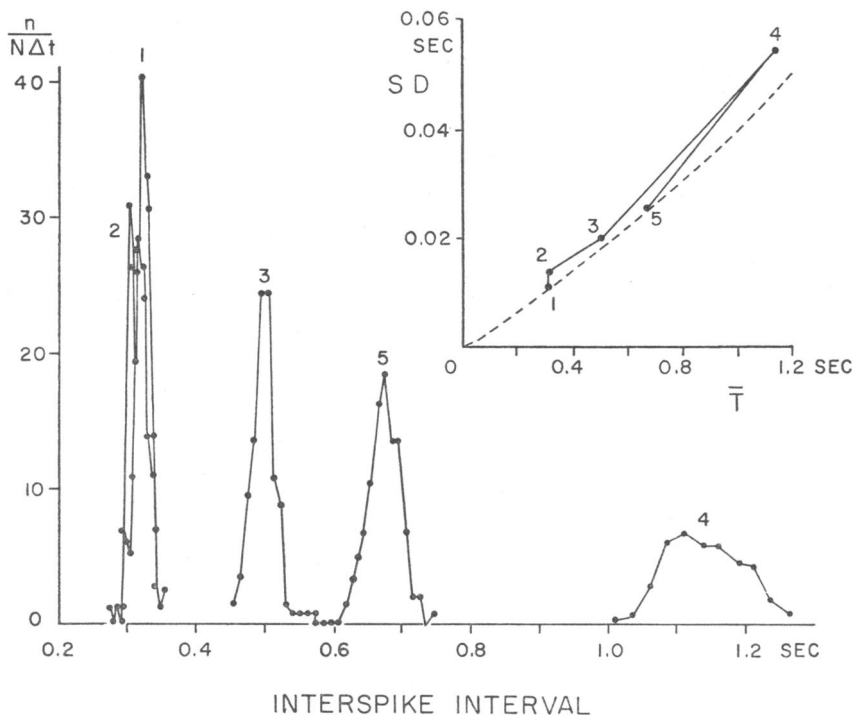
FIGURE 10 Interspike-interval histograms obtained from a single pacemaker neuron, artificially made to fire at different mean rates with dc stimulation through a second somatic electrode. Ordinates given as probability densities, to compensate for difference in sample sizes. 1. Spontaneous; 2. Outward current through cell membrane; 3. Spontaneous, showing aftereffect of slowing due to stimulation in (2); 4. Inward current through cell membrane; 5. Spontaneous. Insert shows standard deviation of the interval histograms vs. mean interval (solid line), compared with SD-mean curve for whole population (dashed line).

Although standard deviation of the interval histograms was strongly correlated with mean for the whole population of cells examined, and for individual cells firing at different mean rates, a certain variability of SD was seen among cells discharging with approximately equal mean intervals. We wished to determine if this variation of SD could be related to differences in the pacemaker potentials from one cell to another. Fig. 11 compares interval histograms and pacemaker potentials of three neurons firing with mean intervals of about 0.65 sec. In parts *a* through *c* the standard deviation increased with decreasing slope of the pacemaker potential just prior to the spike. A similar dependency of interval variability upon potential slope was also seen in another set of cells with common mean rates. This result supports a model where the times of firing are determined by the intersection of curves of membrane potential and threshold. In such a model, for a constant
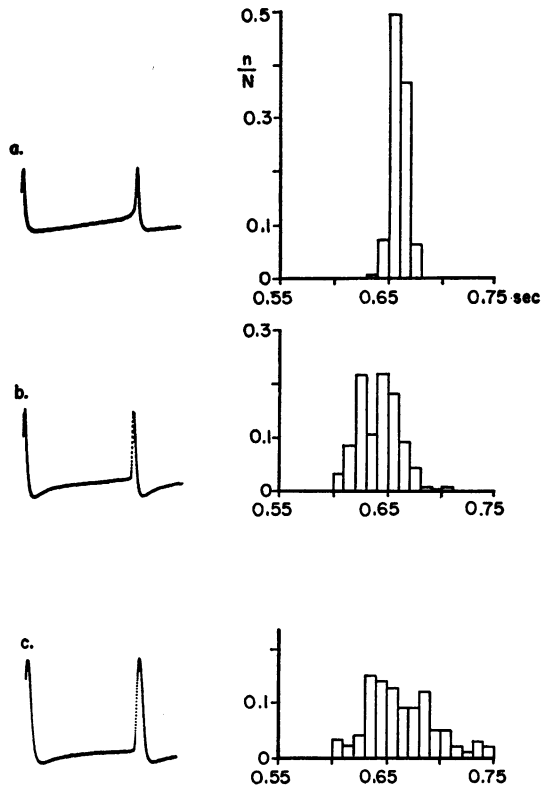
FIGURE 11 Inverse relation of standard deviation of intervals to slope of pacemaker potential just prior to spike, in cells firing with approximately equal mean intervals. Ordinates of interval histograms normalized, to compensate for difference in sample sizes.

amount of fluctuation of potential just before the spike, the slope of the potential is of major importance in determining the SD of intervals. Further details of this model will be presented below.

DISCUSSION

A Physical Model of the Pacemaker Process. In section A of the Results, it was shown that a general description of our directly recorded pacemaker potentials could be provided by exponential curves. However, it should be noted that somatic pacemaker potentials are probably different from those in the spike-initiating region, where the timing of discharges is presumably determined. One model for the sequence of events in a pacemaker neuron is shown in Fig. 12. Some pacemaker locus in the cell presumably acts as a sink for extracellular current. (This locus is shown schematically only, but could represent fine axon terminals, where a
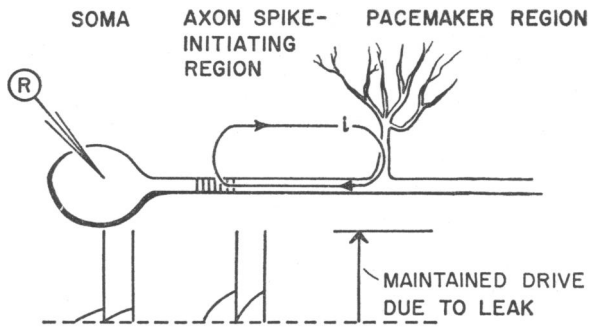
FIGURE 12 Possible mechanism of pacemaker neuron activity. Pacemaker region (shown schematically) acts as a current sink, and exerts a depolarizing drive on all parts of the cell membrane. Axon spike-initiating region, having lowest threshold, is first to discharge. Somatic pacemaker potentials are reduced electrotonically from those in the spike-initiating region. See text for further discussion.

small leakage current would produce a large change in local intracellular ionic concentration.) The pacemaker locus thus exerts a depolarizing drive on all parts of the cell membrane. The axonal spike-initiating region, which is known to have the lowest threshold (Tauc, 1962b), is first to discharge, and axon spikes then invade the soma. If, as shown in Fig. 12, the pacemaker locus is further from the soma than the spike-initiating region, then somatic pacemaker potentials are smaller than those in the spike-initiating region. This geometry has not been definitely established for Aplysia neurons, but at least it is true that no axonal branchings occur between the soma and the spike-initiating region (Tauc, 1962a). It has been suggested (Tauc, 1960) that differences in somatic pacemaker potential size from one cell to another are due to a variable separation of the pacemaker locus from the soma.

The most striking result concerning potential fluctuations in Aplysia cells was the fact that successive pacemaker potentials usually followed different time courses, and did not overlap if superimposed. Most of the single-neuron models to date have treated the membrane noise as a continuous Gaussianlike perturbation of the potential. Following Fatt and Katz (1952), the noise is usually assumed to arise in fine axon terminals and to have the characteristics that (a) its rms value is a constant, independent of the time after a spike, and (b) it is not reset to a certain level or otherwise affected by the spike. These assumptions predict a wide degree of overlap of superimposed interspike potentials, as the model membrane potential fluctuates up and down continuously, with no relation to the time of firing.

The finding of nonoverlapping pacemaker potentials in Aplysia neurons suggests two conclusions: first, since the pacemaker potentials are different from interval to interval, it is reasonable to suppose that the observed fluctuations are due to a discrete once-per-cycle resetting of some parameter. It is natural to attribute the

resetting to the spike itself, since this is the most conspicuously discontinuous event in the cycle. The potential fluctuations are certainly time locked to the spikes, as the standard deviation of potential is always minimum at the undershoot (Fig. 6). Second, once the pacemaker process is reset, it is maintained in its new state *through-out the interval*. Superimposed pacemaker potentials do not differ in certain parts of the cycle and overlap in others; they differ throughout the cycle. In terms of a model of passive charging of the cell membrane, it is as if the charging current reaching the spike-initiating region, or membrane resistance in that region, were randomly reset to a new level by each spike, and maintained at that level until the next spike. Variations in the charging current could reflect a randomly changing position of the spike-initiating region with respect to the pacemaker locus (Tauc, 1962*a*). Membrane resistance, which undergoes an abrupt decrease during the spike (Fessard and Tauc, 1956), might well be reset in a random manner and not to a fixed value. Since our measurements of resistance were in terms of potential levels produced by current pulses, it was not possible to separate fluctuations of resistance from fluctuations already present in the membrane potential. Hence we could not exclude either the hypothesis of fluctuating resistance or fluctuating current as the source of variability of the pacemaker potentials.

Several previous models have assumed that fluctuations of firing threshold contributed to the variability of interspike intervals in single neurons (ten Hoopen, 1964; Buller, 1965; Verveen and Derksen, 1965; Perkel, 1965). "Threshold" as defined for extracellular stimuli has been shown to fluctuate in isolated nerves (Pecher, 1939; Verveen, 1961; Verveen and Derksen, 1965), and in some central neurons (Frishkopf and Rosenblith, 1958). However, evidence that fluctations of threshold contribute much less to the variability of the discharge of our pacemaker neurons than do fluctuations of membrane potential is presented in Fig. 13. If, as shown in Fig. 13*a*, the firing threshold is constant, then the curves of potential must differ *ipso facto* to account for the known irregularity of firing. If, on the other hand, the intervals are determined largely by fluctuations of threshold (Fig. 13*b*), then all the spikes should arise from the same curve of potential. (Of course, intermediate cases are also possible). As previously seen in Fig. 5, the pacemaker potentials in *Aplysia* cells are different from one interval to the next; in general, they look more like Fig. 13*a* than Fig. 13*b*. This suggests that the major variation of intervals in these neurons may be assigned to fluctuations in the time course of membrane potential between spikes.

A Mathematical Model of the Pacemaker Process. As mentioned above, a strong correlation of standard deviation of intervals and mean interval was observed between different spontaneously active cells, and in single cells firing at different mean rates. This could be explained conceptually by a one-parameter model (that is, where only one parameter was assumed to vary from cell to cell). We wished to test such a model quantitatively. The question asked was whether, by assuming reasona-
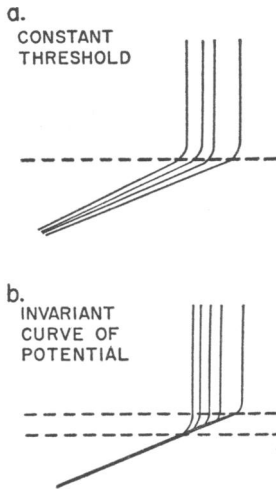
FIGURE 13 Comparison of "constant threshold" and "invariant potential" models of spike initiation. Part *a*. Constant firing threshold indicated by dotted line. Superimposed pacemaker potentials must differ in the time course of charging to the threshold level, to explain the known irregularity in time of firing. Part *b*. Successive spikes arise from identical curves of potential. Fluctuations of threshold, indicated by dotted lines, produce the irregularity of firing. Further discussion in text.

ble or directly measured values of the different cell parameters, the model could accurately predict the observed form and variation of interspike-interval histograms. In the interest of permitting a clear physiological interpretation of each parameter, the model was formulated as simply as possible.

Those characteristics of the real interval histograms which we felt the simulation should describe were the following: (*a*) the discharges were quite regular; i.e., coefficients of variation were less than 0.08. (*b*) Interval histograms were unimodal with mean values close to the modes. Skewness was small. (*c*) Standard deviation of intervals varied with mean interval according to the function $\text{SD} = 0.00944 \, (\bar{T})^{1.21}$. (This describes the variation from one cell to another, as shown in Fig. 9, and approximates that seen in the single cell of Fig. 10.)

The model is shown in Fig. 14. It is one version of a previously published simulation program for the IBM 7094 computer (Perkel, 1965). Following each spike, the membrane potential, indicated by the heavy line, is undefined for a period ρ, the "absolute refractory period." It is then reset to an invariant value, the "undershoot," and it decays positively along an exponential curve: $V = V_R(1 - e^{-t/\tau})$, where t is the time since the undershoot. The next spike occurs when the potential exceeds the threshold value, which is V_T mv less negative than the undershoot. Fluctuations of interval length are introduced by choosing V_R, the asymptotic potential measured from the undershoot, from a normal population with mean $\bar{V}_R$ and standard devia-
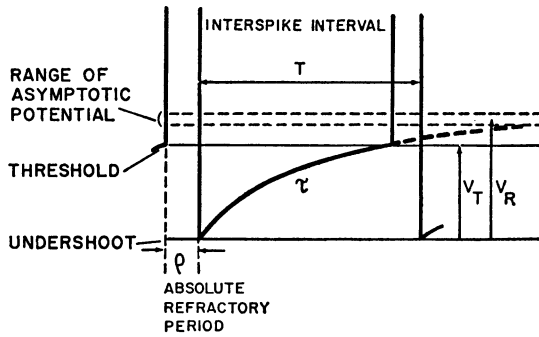
FIGURE 14. Mathematical model of the pacemaker process. Membrane potential indicated by heavy line. Spike (vertical heavy lines) is produced when membrane potential reaches threshold. Pacemaker potential assumed to be exponential, with time constant $= \tau$. Fluctuations of interspike intervals produced by choosing asymptotic potential, following each spike, from a normal population. Further discussion in text.

tion σ. We can approximate the mean interval, $\bar{T}$, by setting $V_R = \bar{V}_R$, and finding the time at which $V = V_T$. This gives

$$V_T = \bar{V}_R[1 - e^{-(T-\rho)/\tau}]$$

which can be solved for $\bar{T}$ as

$$\bar{T} = \rho + \tau \ln \frac{\bar{V}_R}{\bar{V}_R - V_T}.$$

It is easily shown (see Appendix) that the probability density function of the resulting interspike intervals is

$$f(t) = \frac{V_T}{\tau\sigma\sqrt{2\pi}} \frac{e^{-(t-\rho)/\tau}}{[1 - e^{-(t-\rho)/\tau}]^2} \exp\left[-\frac{1}{2\sigma^2}\left(\frac{V_T}{1 - e^{-(t-\rho)/\tau}} - \bar{V}_R\right)^2\right]$$

The shape of this function will be illustrated by the results of the simulation.

Fig. 15 shows an attempt to model the variations of interval histograms throughout the population of pacemaker neurons. Five different cases were simulated, covering a wide range of mean firing rates. In Fig. 15b, pacemaker potentials are shown corresponding approximately to mean intervals for each case. The absolute refractory period, ρ, had a constant value of 0.025 sec, which is a typical spike width in *Aplysia* cells (see Fig. 3). The time constant, τ, was 1.44 sec in each case (this cannot be measured exactly in the spike initiating region). V_T, the firing threshold measured from the undershoot, was a constant 15 mv. Since we would not expect σ, the standard deviation of asymptotic potential, to be constatn from one case to the next, we assumed equal values of SD_V, the standard deviation of potential just before the spike (indicated by broken line). The model SD_V was 0.4 mv, which fell within the range of measured values (Fig. 6). The only parameter assumed to vary was $\bar{V}_R$, the mean asymptotic potential.

This model duplicates two special characteristics of pacemaker potentials observed in real cells: (a) Since V_R, the asymptotic potential measured from the undershoot, is restored to a random level after each spike and held constant until the next spike, successive pacemaker potentials are different throughout the cycle. They would not overlap if superimposed. (b) The standard deviations of the model histograms vary inversely with the mean slopes of the pacemaker potentials at the time of firing.

The interspike-interval histograms resulting from each assumed value of $\bar{V}_R$ are shown in Fig. 15a. These resembled the histograms obtained from real cells in that (a) they had small coefficients of variation (0.025 to 0.082), (b) they were unimodal and had small values of skewness (0.150 to 0.416), and (c), as shown in Fig. 15c, the observed variation of SD with mean interval was followed over a large range of firing rates.

It should be noted that the correlation of SD of intervals and mean interval in the model does not follow uniquely from variations of the asymptotic potential, but will also result if the firing threshold, V_T or the time constant, τ is allowed to vary. However, the variable threshold model predicts that the fastest cells should have the lowest thresholds, measured from the undershoot; as mentioned previously, some of the largest values of V_T in somatic records occurred at the smallest mean intervals. The variable time constant model was rejected because of the difficulty of physical interpretation: if only the time constant, τ, was assumed to vary, then the observed curve of SD vs. $\bar{T}$ could be fitted. However, since the asymptote of potential is presumably related to the membrane resistance, then for τ only to vary, resistance must be assumed constant, and membrane capacity must vary. If only the resistance varied, then cells with the largest time constants would also have the greatest asymptotes of potential. This case could not predict the observed relation of SD vs. mean interval. A sufficient and much simpler explanation was given by the model of varying asymptotic potential presented above. In this view, the differences between pacemaker potentials may easily be attributed to the amount of current drive reaching the spike-initiating membrane, perhaps depending on its separation from the pacemaker locus. In the case of single cells subjected to dc stimulation, the applied current sums with or subtracts from the maintained current due to the pacemaker leak. This moves the discharge up or down and SD-mean curve which differs from the average curve for the spontaneously active population only in small variations of other cell parameters (σ, τ, V_T).

This work represents an initial attempt to explain single neuron discharges quantitatively in terms of directly measurable cell parameters, and we feel that it points out the need for further studies in this direction. Certainly it will be possible to determine the sources of interspike-interval fluctuations in other invertebrate preparations which permit intracellular recording, and where the data are not complicated by synaptic input (Fuortes and Mantegazzini, 1962; Eyzaguirre and Kuffler, 1955). In preparations where input is present, one task will be to relate quantitatively the statistics of the spike discharge to the temporal distribution of synaptic events (see, for instance,

a.

c.

INTERVAL

b.

TIME
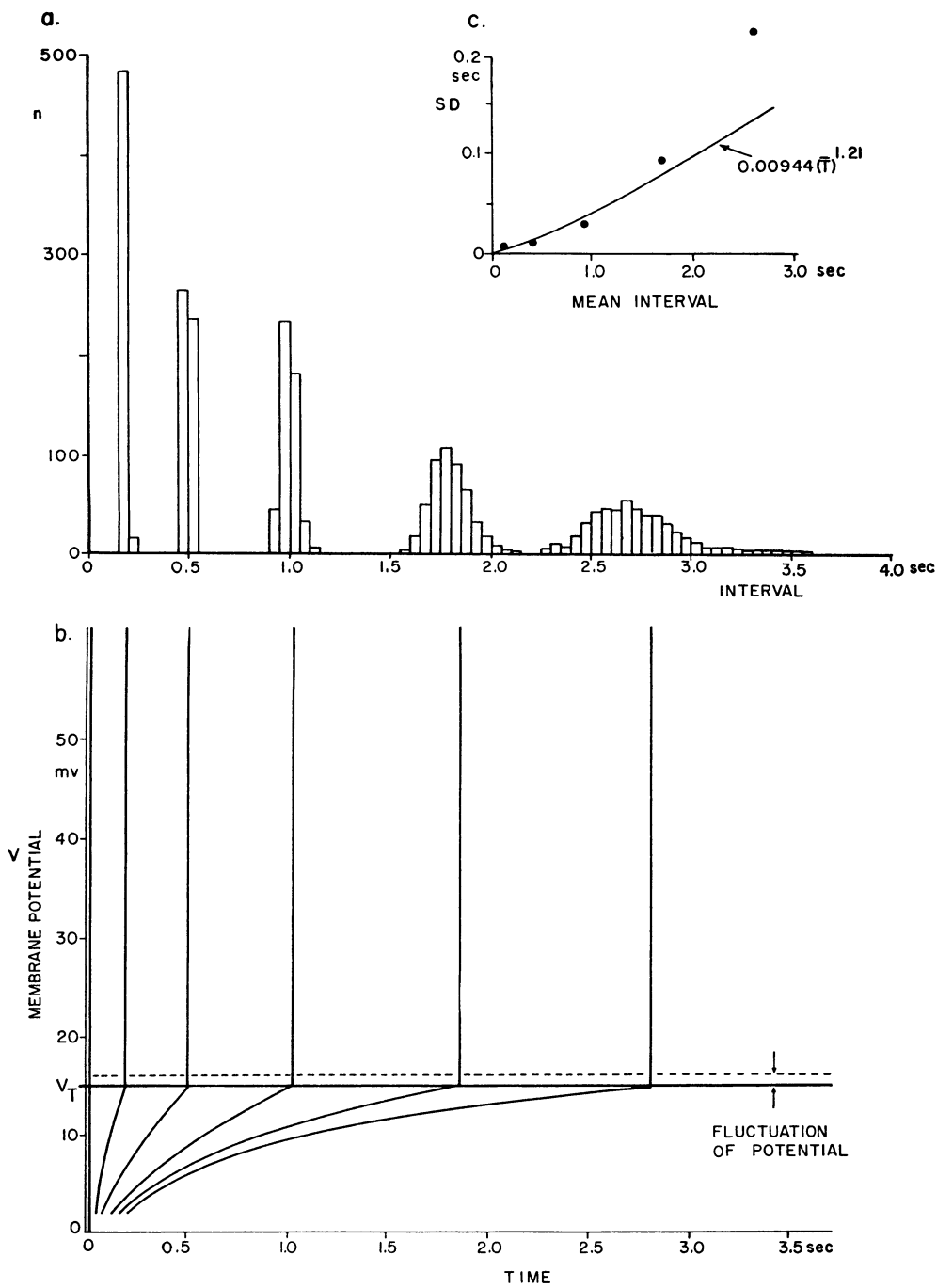
Segundo et al., 1966). The development of electrophysiological techniques should by now permit the testing of theoretical single-neuron models against direct intracellular data.

APPENDIX

Probability Density Function of Interspike Intervals from the Model. The interspike interval, T, is a monotonically decreasing function of the random variable V_R, in the range $V_R > V_T$:

$$T = H(V_R) = \rho + \tau \ln \frac{V_R}{V_R - V_T}$$

Since we assume that V_R is normally distributed, with probability density function

$$g(v_R) = \frac{1}{\sigma\sqrt{2\pi}} \exp\left[-\frac{1}{2\sigma^2}(v_R - \bar{v}_R)^2\right],$$

we can find $f(t)$, the probability density function for T, as follows (Hoel, 1962, p. 121):

$$f(t) = -g[h(t)]h'(t),$$

where $h(T)$ is the inverse of $H(V_R)$, and $h'(T)$ is its derivative:

$$h(T) = \frac{V_T}{1 - e^{-(T-\rho)/\tau}}$$

$$h'(T) = -\frac{V_T}{\tau} \frac{e^{-(T-\rho)/\tau}}{[1 - e^{-(T-\rho)/\tau}]^2}$$

Thus,

$$f(t) = \frac{V_T}{\tau\sigma\sqrt{2\pi}} \frac{e^{-(t-\rho)/\tau}}{[1 - e^{-(t-\rho)/\tau}]^2} \exp\left[-\frac{1}{2\sigma^2}\left(\frac{V_T}{1 - e^{-(t-\rho)/\tau}} - \bar{V}_R\right)^2\right]$$

FIGURE 15 Simulation of the variation of interspike-interval histograms from one spontaneously active cell to another, based on the model in Fig. 14. Part *b*. Curves of membrane potential corresponding approximately to the mean interval in each of the five cases simulated. Only asymptotic potential, measured from the undershoot, was assumed to vary from case to case. See text for details. Part *a*. Histograms of 500 intervals for each of the model cases. Part *c*. Variation of standard deviation of model histograms with mean interval, shown by dots. Solid line shows power function describing observed variation of SD with mean interval in spontaneously active pacemaker neurons.

REFERENCES

AMASSIAN, V. E., MACY, J., WALLER, H. J., LEADER, H. S., and SWIFT, M., 1962, *Proc. Internat. Union Physiol. Sc., 22nd Congress Leiden*, **3**, 235.

ARVANITAKI, A., and CHALAZONITIS, N., 1958, *J. Physiol. Paris*, **50**, 122.

BIEDERMAN, M. A., 1965, On the nature and sources of spontaneous activity in the isolated crayfish abdominal nerve cord, U.C.L.A. Dept. of Zoology, Ph.D. dissertation.

BISHOP, P. O., LEVICK, W. R., and WILLIAMS, W. O., 1964, *J. Physiol.*, **170**, 598.

BULLER, A. J., 1965, *J. Physiol.*, **179**, 402.

CALVIN, W. H., and STEVENS, C. F., 1965, *Physiologist*, **8**, 127.

COX, D. R., and LEWIS, P. A. W., 1966, The Statistical Analysis of Series of Events, London, Methuen and Co., Ltd.

EYZAGUIRRE, C., and KUFFLER, S. W., 1955, *J. Gen. Physiol.*, **39**, 87.

FATT, P., and KATZ, B., 1952, *J. Physiol.*, **117**, 109.

FELLER, W., 1957, An Introduction to Probability Theory and its Applications, New York, John Wiley & Sons, 278.

FESSARD, A., and TAUC, L., 1956, *J. Physiol. Paris*, **48**, 541.

FETZ, E. E., and GERSTEIN, G. L., 1963, *Quart. Prog. Report, M.I.T. Research Lab. Elect.*, **71**, 249.

FRISHKOPF, L. S., and ROSENBLITH, W. A., 1958, in Symposium on Information Theory in Biology, New York, Pergamon Press Limited, 153.

FUORTES, M. G. F., and MANTEGAZZINI, F., 1962, *J. Gen. Physiol.*, **45**, 1163.

GEISLER, C. D., and GOLDBERG, J. M., 1966, *Biophysic. J.* **6**, 53.

GERSTEIN, G. L., and MANDELBROT, B., 1964, *Biophysic. J.*, **4**, 41.

GOLDBERG, J. M., ADRIAN, H. O., and SMITH, F. D., 1964, *J. Neurophysiol.*, **27**, 706.

HAGIWARA, S., 1954, *Japan. J. Physiol.*, **4**, 234.

HOEL, P. G., 1962, Introduction to Mathematical Statistics, 3rd edition, New York, John Wiley & Sons.

LEWIS, E. R., 1965, *J. Theoret. Biol.*, **10**, 125.

MOORE, G. P., PERKEL, D. H., and SEGUNDO, J. P., 1966, *Ann. Review Physiol.*, **28**, 493.

PECHER, C., 1939, *Arch. Internat. Physiol.*, **49**, 129.

PERKEL, D. H., 1965, in Biophysics and Cybernetic Studies, (M. Maxfield, A. Callahan, and L. J. Fogel, editors), Washington, D. C., Spartan Books, 37.

SEGUNDO, J. P., PERKEL, D. H., and MOORE, G. P., 1966, *Kybernetik*, **4**, 67.

STEIN, R. B., 1965, *Biophysic. J.*, **5**, 173.

TAUC, L., 1960, *Compt. Rend. Soc. Biol.*, **154**, 17.

TAUC, L., 1962a, *J. Gen. Physiol.*, **45**, 1077.

TAUC, L., 1962b, *J. Gen. Physiol.*, **45**, 1099.

TEN HOOPEN, M., 1964, *Japan. J. Physiol.*, **14**, 607.

TEN HOOPEN, M., 1966, *Kybernetik*, **3**, 17.

TOKIZANE, T., and SHIMAZU, H., 1964, Functional Differentiation of Human Skeletal Muscle. Tokyo, University of Tokyo Press.

VERVEEN, A. A., 1961, Fluctuation in Excitability, Drukkerij Holland N.V., Amsterdam.

VERVEEN, A. A., and DERKSEN, H. E., 1965, *Kybernetik*, **2**, 152.

VIERNSTEIN, L. J., and GROSSMAN, R. G., 1961, in Information Theory, Fourth London Symposium, London, Butterworth & Co., 252.

WEAST, R. C., editor, 1964-65, Handbook of Chemistry and Physics, Cleveland, Chemical Rubber Co., A-163.

WEISS, T. F., 1964, *M.I.T. Research Lab. Elect. Tech. Report No. 418*.

WERNER, G., and MOUNTCASTLE, V. B., 1963, *J. Neurophysiol.*, **26**, 958.